LOCKED MODES AND PLASMA-WALL INTERACTION IN A REVERSED-FIELD PINCH WITH A RESISTIVE SHELL AND CARBON FIRST WALL

S. HOKIN [a], H. BERGSÅKER [a], P. BRUNSELL [a], J. BRZOZOWSKI [a], M. CECCONELLO [a], J. DRAKE [a], G. HEDIN [a], A. HEDQVIST [b], D. LARSSON [c], A. MÖLLER [a], E. SALLANDER [a], H.-E. SÄTHERBLOM [a]

[a]Division of Fusion Plasma Physics, Alfvén Laboratory
[b]Department of Physics I
[c]Department of Physics Frescati
Association Euratom-NFR, Royal Institute of Technology, S-100 44 Stockholm, Sweden

Introduction. The Extrap-T2 reversed-field pinch has concluded operation in the OHTE RFP configuration with a resistive shell. T2 is the only RFP that has recently operated with a resistive shell: $\tau_{\text{shell}} \simeq 1.5$ ms, which is much shorter than the pulse duration of up to 15 ms. The minor radius of the shell is $b = 1.09a$, where $a = 18.3$ cm is the radius of the first wall. The wall is covered by carbon tile armor. This paper summarizes our observations and conclusions regarding wall-locked modes, dynamo activity and plasma-wall interaction (PWI) with a resistive shell and graphite first wall.

Measurements indicate that plasma performance is significantly degraded by the presence of a toroidally-localized, wall-locked, internally-resonant mode, despite the fact that discharge duration of up to ten times the shell penetration time can be achieved. 3-D resistive MHD simulations demonstrate the degradation of magnetic topology which occurs with a resistive shell. A new observation is that high frequency dynamo activity originates in the region of the locked mode, contributing to an asymmetry of toroidal flux. The distorted flux surfaces give rise to regions of very intense power loads on the graphite first wall, resulting in impurity and hydrogen release. A hydrogen recycling and fueling model simulates the rise of density observed in PWI events, due to thermal H release when the graphite surface temperature exceeds 1000 K. Infrared camera measurements show that at regions of intense PWI, the wall temperature reaches up to 1200 K by the end of the discharge. The total area of these regions is estimated from camera pictures to be approximately 2% of the total first wall area. This result is in agreement with the hydrogen recycling model where local heating of 2–5% of the first wall area can reproduce the experimentally observed density evolution. In addition, carbon and oxygen are released into the plasma, further cooling the electrons, increasing Z_{eff} and leading to increased plasma resistance. A 1-D transport code predicts that there could be improvement of energy confinement by at least a factor of three with reduction of the locked mode to below the level of the existing temporal fluctuations.

Wall-Locked Modes. T2 is equipped with an array of 32 loops which measure the toroidal flux within the outer radius of the toroidal field coils and a 4×32 array of pickup coils which measure the radial magnetic field B_r at the outer surface of the shell. These have been used to diagnose the wall-locked mode which grows on the resistive shell penetration time-scale in every discharge.

The mode manifests itself on both magnetic diagnostics: as a localized increase (typically 10%) of toroidal flux and as a localized region with a large radial field ($B_r/B \simeq 5\%$). Fig. 1 displays the distortion of an outer poloidal flux surface constructed using the poloidal field data. Although the narrow toroidal extent of the mode makes accurate mode analysis difficult, the measurements indicate that the mode is internally resonant, with poloidal mode number $m = 1$ and a broad n spectrum centered around

$n = 12 \simeq 2R/a$. The mode is therefore a wall-locked version of the internal tearing mode 'slinky' seen on many RFP devices. External, low-n 'resistive-shell' modes are, if present, obscured by external field errors. The locking location varies from discharge to discharge, and is likely associated with external field errors which provide a nonzero seed B_r at the edge. Locking can be forced at the location of an externally-applied $m = 1$ field error [1].

Simulations carried out with the DEBS [2] resistive MHD code using a resistive-shell boundary condition, but low aspect ratio ($R/a = 2.2$), show similar behavior, with a $\pm$20% toroidal variation of the toroidal flux and a local region where B_r/B reaches 20%. As shown in Fig. 2, the mode degrades the magnetic geometry in the outer half of the plasma and makes the reversal surface extend outside the shell along an $m = 1$ band over a 90° toroidal extent. Although T2 has much higher aspect ratio ($R/a = 6.8$), and therefore a more localized mode structure, the DEBS simulation provides a good qualitative picture of the locked-mode topology.

Dynamo Activity and Confinement. Toroidally localized flux generation occurs largely in discrete events in the region of the locked mode, with a period of 100–150 μs. These local dynamo events appear at the position of the wall-locked mode and rotate toroidally around the torus, diffusing and reconnecting in less than one turn, yielding an axisymmetric toroidal flux contribution. Similar events have been observed in ZT-40 and are therefore not a resistive-shell feature. However, in T2 the fixed starting position of the events creates a stationary toroidal flux perturbation at the position of the wall-locked mode. In addition, the dynamo activity is correlated with coherent $n = 0$ oscillations in soft x-ray emission, and occasionally with edge localized line emission in the locked mode region. This suggests that the core electron temperature and the edge particle flux is modulated by localized dynamo activity. We conclude that a large fraction of dynamo activity is associated with the locked mode and affects global confinement.

Plasma-Wall Interaction and Confinement. The wall-locked mode leads to a localization of power flux and, to a lesser extent, particle flux to the wall, often resulting in a strong influx of hydrogen and impurities along with a characteristic drop of the edge electron temperature from 20 to 5 eV. Calorimeter probe measurements indicate that, on average, heat flux in the range 15–45 MW$\cdot$m^{-2} is incident in the electron drift direction on the exposed edges of the graphite tiles in 150-kA discharges.

A fast (1 ms/frame) and a slow (20 ms/frame) CCD camera have been used to obtain photographic images of the first wall. The camera view is along a tangential chord and covers a $\Delta\phi = 50^\circ \pm 10^\circ$ toroidal sector. Fig. 3 displays an image of H_α ($\lambda = 6560 \pm 65$ Å) line radiation obtained with the fast camera in which the wall-locked mode is evident as a region of greatly-enhanced emission. The region has an $m = 1$ structure, $n = 12 - 18$ with a pitch coinciding with the helicity of the internally-resonant modes. The $m = 1$ instability is a common feature and characterized by a full turn in the poloidal direction. The typical toroidal width of the structure is about 20°.

Using a CII camera filter ($\lambda = 5150 \pm 25$ Å), similar $m = 1$ structures are observed. In addition, local hot-spots have been observed with high poloidal mode number ($m \sim 6$). Typical effects of carbon blooming with sudden increase of carbon impurity influxes have also been observed at the end of the discharges. Infrared measurements ($\lambda = 10240 \pm 150$ Å) with the slow camera show that temperatures exceeding 1200 K are reached on a small fraction of the graphite wall ($> 1\%$ of the total area) during the discharge. This is sufficient for thermal release of trapped hydrogen (900 K) and for self-sputtering and chemical erosion of the graphite-wall.

In Fig. 4, the density evolution for a 180-kA discharge, which exhibited a rapid density increase due to a plasma-wall interaction event, is overlayed with a hydrogen recycling and fueling simulation assuming 2–5% of the surface is affected by thermal release of trapped particles. The same discharge has been analyzed with calibrated VUV spectroscopy, showing that the strong increase of density at

$t = 4.5$ ms (Fig. 4) is accompanied by increases of impurity line emission and plasma resistance. The increase of plasma resistance is within the range calculated using Spitzer resistivity and the observed drop of core T_e from 100 to 50 eV and increase of Z_{eff} from 1.9 to 3.6. The Z_{eff} rise is due in large part to increased carbon concentration. The global energy confinement time decreases by 40% (assuming equal ion and electron energy content). The plasma partially recovers from the strong hydrogen and impurity influx: n_e and Z_{eff} decrease while T_e increases somewhat, resulting in continuation of the discharge in a colder, more resistive, state.

Transport Simulations. The 1-D particle/energy/neutral transport code RFPEQ [3] has been used to compare two cases: an experimental 150-kA discharge condition with a locked mode perturbation $B_r/B = 4.5\%$, and a hypothetical discharge with $B_r/B = 2.0\%$, corresponding to the measured level of temporal fluctuations. This gives an estimate of the minimum improvement one would achieve by eliminating the locked mode either with a conducting shell or active control such as forced rotation. The neutral density was adjusted to maintain equal plasma density (2×10^{19} m^{-3}). This comparison suggests that elimination of the locked mode would increase T_{e0} from 80 to 140 eV and reduce the loop voltage from 100 to 50 V, increasing the global energy confinement time by a factor of three in addition to improvements expected from reduced plasma-wall interaction.

Conclusions. Measurements on Extrap-T2 with a graphite wall and resistive shell indicate that plasma performance is significantly degraded by the presence of a wall-locked, internally-resonant mode, despite the fact that discharge duration of up to ten times the shell penetration time can be achieved. 3-D resistive MHD simulations demonstrate the degradation of magnetic topology which occurs with a resistive shell. Impulsive dynamo activity originates in the region of the locked mode, contributing to an asymmetry of toroidal flux. This asymmetry is well established before flat-top conditions are reached, suggesting that τ_{shell} is too short as compared to the time-scale for tearing-mode growth and the related dynamo and relaxation phenomena. Therefore the wall-locking prohibits establishment of good RFP equilibrium. A hydrogen recycling and fueling simulation matches the rise of density observed in PWI events with thermal H release when 2–5% of the graphite surface is heated to 1000 K. In addition, carbon and oxygen are released into the plasma, further cooling the electrons, increasing Z_{eff} and leading to increased plasma resistance. A 1-D transport code predicts improvement of energy confinement by at least a factor of three with reduction of the locked mode to well below the existing temporal fluctuation levels.

T2 Rebuild. T2 is now being rebuilt with several significant changes: (1) the single-layer brass shell is replaced by an overlapping double-layer copper shell with a shell penetration time of 5 ms; (2) the graphite first wall is replaced by a large number of molybdenum mushroom limiters; (3) a new vacuum chamber allows increased diagnostic access; (4) the helical toroidal field coil is replaced by a conventional 64-coil solenoid. Unlike the previous T2 configuration, in which the plasma current ramp time (2.5 ms) was longer than the shell time (1.5 ms), allowing the locked mode to develop during the period of strong ramp-up dynamo activity, the T2 rebuild will reach maximum current on a time scale corresponding to conducting-shell boundary condition. This allows one to study the transition from conducting shell to resistive shell equilibrium with improved plasma conditions. The rebuilt device will begin operation in 1999.

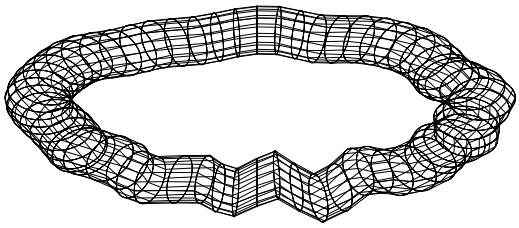

FIG. 1. The poloidal flux surface at the radius of the resistive shell, generated from radial field measurements at time $t = 7$ ms in a discharge, when the wall-locked mode is fully developed. (Distortions are magnified by a factor of 10.)

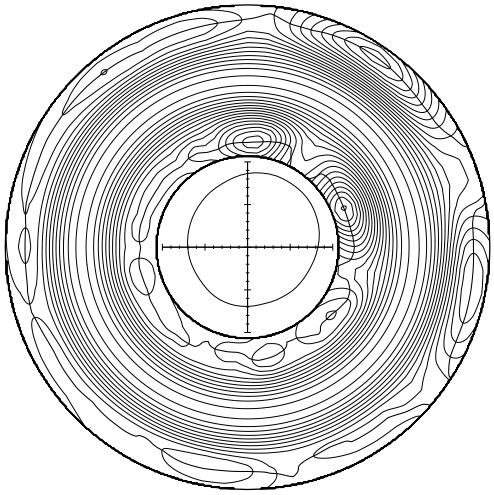

FIG. 2. Midplane toroidal flux contours from a DEBS resistive-shell simulation at aspect ratio 2.2. The contours indicate the position of field lines as they cross the midplane. The reversal surface is shown with a darker internal line. The total toroidal flux is shown on the inner polar plot.

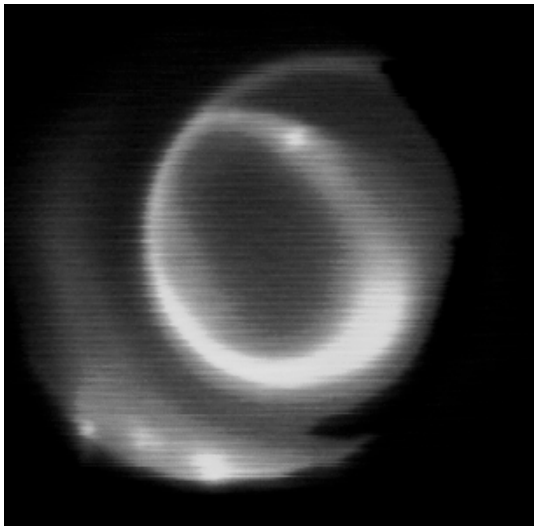

FIG. 3. An image of H_α line emission obtained with a camera viewing along a tangential chord. The wall-locked mode is visible as a region of enhanced emission with an $m = 1$ mode structure.

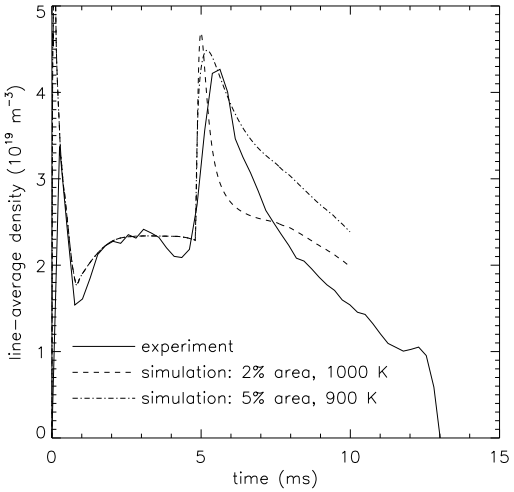

FIG. 4. Line-average electron density from a T2 shot with a strong plasma-wall interaction event, along with two simulations of hydrogen recycling and fueling which include a sudden temperature increase on a small fraction of the surface area at $t = 4.8$ ms.

[1] G. Hedin, Proc. 20th EPS Conf. on Cont. Fusion and Plasma Physics, Vol. III, 1265 (1997).
[2] D. Schnack and S. Ortolani, Nucl. Fusion **30**, 277 (1990).
[3] S. Hokin, Nucl. Fusion **37**, 1615 (1997).